

# Two Photon Exchange Contributions to Elastic $\bar{e} + p \rightarrow e + \bar{p}$ Process in a Nonlocal Field Formalism

Pankaj Jain, Satish D. Joglekar and Subhadip Mitra

Department of Physics, IIT Kanpur, Kanpur - 208016, India

**Abstract:** We compute the two photon exchange contributions to elastic scattering of polarized electrons from target protons. We use a nonlocal field theory formalism for this calculation. The formalism maintains gauge invariance and provides a systematic procedure for making this calculation. The results depend on one unknown parameter  $\bar{b}$ . We compute the two photon exchange correction to the ratio of electric to magnetic form factors extracted using the polarization transfer experiments. The correction is found to be small if  $\bar{b} \sim 1$ . However for larger values of  $\bar{b} > 3$ , the correction can be quite significant. The correction to the polarization transfer results goes in the right direction to explain their difference with the ratio measured by Rosenbluth separation method. We find that the difference between the two experimental results can be explained for a wide range of values of the parameter  $\bar{b}$ . We also find that the corrections due to two photon exchange depend on the photon longitudinal polarization  $\varepsilon$ . Hence we predict an  $\varepsilon$  dependence of the form factor ratio extracted using the polarization transfer technique. Finally we obtain a limit on  $\bar{b}$  by requiring that the non-linearity in  $\varepsilon$  dependence of the unpolarized reduced cross section is within experimental errors.

## 1 Introduction

The observed discrepancy [1, 2] in the proton electromagnetic form factors in the JLAB polarization transfer experiments [3, 4, 5, 6] and the SLAC Rosenbluth separation experiments [7, 8, 9] has been studied extensively in the literature. The two photon exchange contributions are most likely the source of the difference [10, 11, 12, 13, 14, 15]. In a recent paper we constructed a nonlocal Lagrangian to model the electromagnetic interaction of extended objects such as the proton [16]. The model maintains gauge invariance in the presence of a form factor at the electromagnetic vertex. We truncate the Lagrangian to include only operators with dimension five or less. The dimension five operator is necessary if we include the contribution proportional to the Pauli form factor  $F_2$ . This truncation is reliable as long as the off-shellness of the proton propagator is small compared to the hadronic momentum scale. The resulting Lagrangian depends on the two on-shell form factors,  $F_1$  and  $F_2$ , and contains one unknown parameter which we denote as  $\bar{b}$ . We found that for small values of this parameter  $\bar{b} \sim 1$ , the results of the SLAC Rosenbluth measurement, after the two photon exchange correction, are in agreement with the JLAB polarization transfer results. In the present paper we compute the two photon exchange corrections to the polarization transfer experiment.

In polarization transfer experiments, longitudinally polarized electrons are scattered from fixed target protons. The tree level amplitude for the process (See Fig. 1) is

given by:

$$\mathcal{M}_0 = -\frac{e^2}{q^2} \bar{u}(k') \gamma^\mu u(k, s_e) \bar{U}(p', s_{p'}) \Gamma_\mu U(p), \quad (1)$$

where

$$\Gamma_\mu = F_1(q) \gamma_\mu + \frac{i\kappa_p}{2M_p} F_2(q) \sigma_{\mu\alpha} q^\alpha. \quad (2)$$

Here  $e$  is the charge of proton,  $k, k'$  are the momenta of the initial and final electron,  $p, p'$  are the initial and final proton momenta,  $M_p$  is the proton mass,  $\kappa_p = 1.79$  is proton anomalous magnetic moment and  $q = p' - p = k - k'$  is the momentum transfer.

Using (1), one can calculate the tree level cross-section for the scattering of longitudinally polarized electrons from protons:

$$\frac{d\sigma^{1\gamma}}{d\Omega_e} = \frac{|\overline{\mathcal{M}}_0|^2 E_e'^2}{64M_p^2 \pi^2 E_e^2}, \quad (3)$$

where  $|\overline{\mathcal{M}}_0|^2$  represents the amplitude squared, summed over final electron spin and averaged over initial proton spin and is given by:

$$\begin{aligned} |\overline{\mathcal{M}}_0|^2 &= \frac{1}{2} \sum_{s'_e, s_p} |\mathcal{M}_0|^2 \\ &= \frac{e^4}{8q^4} \text{tr} \left[ (\not{k} + m_e) \left( 1 + \frac{\hbar}{m} \gamma_5 \not{k} \right) \gamma^\nu (\not{k}' + m_e) \gamma^\mu \right] \\ &\quad \times \text{tr} \left[ (\not{p} + M_p) \gamma_0 \Gamma_\nu^\dagger \gamma_0 (\not{p}' + M_p) \left( 1 + \gamma_5 \not{p}' \right) \Gamma_\mu \right]. \end{aligned} \quad (4)$$

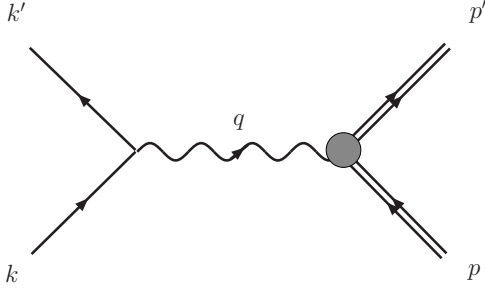


Figure 1: The one photon exchange diagram contributing to the elastic electron proton scattering. Here  $k, k'$  refer to the initial and final electron momenta and  $p, p'$  to the initial and final proton momenta respectively. The symbol  $q = k - k' = p' - p$  denotes the momentum exchanged.

Here  $s_{p'}^\mu$  is the spin four-vector of the final proton. In general the spin four-vector  $s$  for a particle with mass  $m$  and momentum  $p = (E; \vec{p})$  can be written in terms of the unit three-vector  $\hat{n}$ , specifying the spin direction in the rest frame of the particle, by

$$s^\mu = \left( \frac{\hat{n} \cdot \vec{p}}{m}; \hat{n} + \vec{p} \frac{\hat{n} \cdot \vec{p}}{m(m+E)} \right). \quad (5)$$

For the incident electron, energy  $E_e$  is much greater than its mass  $m_e$ , and we have approximated the spin four vector,  $s_e^\mu \approx h k^\mu / m_e$ , where  $h = \hat{n}_e \cdot \hat{k}$ .

Let the scattering plane be the  $X - Z$  plane where the momentum of the recoiled proton  $\vec{p}'$  defines the  $Z$  axis, i.e.,  $\hat{z} = \hat{p}'$ . The  $Y$  axis is defined as  $\hat{y} = \hat{k} \times \hat{k}'$ . This also defines the  $X$  axis as  $\hat{x} = \hat{y} \times \hat{z}$ . With this choice of coordinate axes, the tree level cross section can be written as:

$$\frac{d\sigma^{1\gamma}}{d\Omega_e} = \left( \frac{\alpha^2 E'_e \cos^2 \frac{\theta_e}{2}}{8E_e^3 \sin^4 \frac{\theta_e}{2}} \right) \left( \frac{1}{1+\tau} \right) \times \left[ I_0^{1\gamma} + h I_0^{1\gamma} P_L^{1\gamma} (\hat{n}_{p'} \cdot \hat{z}) + h I_0^{1\gamma} P_T^{1\gamma} (\hat{n}_{p'} \cdot \hat{x}) \right], \quad (6)$$

where

$$\begin{aligned} I_0^{1\gamma} &= G_E^2 + \frac{\tau}{\varepsilon} G_M^2, \\ I_0^{1\gamma} P_L^{1\gamma} &= \frac{E_e + E'_e}{M_p} \sqrt{\tau(1+\tau)} G_M^2 \tan^2 \frac{\theta_e}{2}, \\ I_0^{1\gamma} P_T^{1\gamma} &= -2\sqrt{\tau(1+\tau)} G_M G_E \tan \frac{\theta_e}{2}. \end{aligned}$$

Here  $\tau = -q^2/4M_p^2$ ,  $\varepsilon = 1/[1 + 2(1 + \tau) \tan^2(\theta_e/2)]$  is the longitudinal polarization of the photon and  $\theta_e$  is the electron scattering angle.  $I_0^{1\gamma}$  is proportional to the tree level unpolarized cross-section.  $I_0^{1\gamma} P_L^{1\gamma}$  ( $I_0^{1\gamma} P_T^{1\gamma}$ ) is proportional to the term in the tree level cross-section that corresponds to scattering a longitudinally polarized electron from an unpolarized proton producing a longitudinally (transversely)

polarized recoiling proton. Let us define,

$$\frac{d\sigma_0^{1\gamma}}{d\Omega_e} = \left( \frac{\alpha^2 E'_e \cos^2 \frac{\theta_e}{2}}{8E_e^3 \sin^4 \frac{\theta_e}{2}} \right) \frac{I_0^{1\gamma}}{1+\tau}, \quad (7)$$

$$\frac{d(\Delta\sigma_L^{1\gamma})}{d\Omega_e} = \left( \frac{\alpha^2 E'_e \cos^2 \frac{\theta_e}{2}}{8E_e^3 \sin^4 \frac{\theta_e}{2}} \right) \frac{I_0^{1\gamma} P_L^{1\gamma}}{1+\tau}, \quad (8)$$

$$\frac{d(\Delta\sigma_T^{1\gamma})}{d\Omega_e} = \left( \frac{\alpha^2 E'_e \cos^2 \frac{\theta_e}{2}}{8E_e^3 \sin^4 \frac{\theta_e}{2}} \right) \frac{I_0^{1\gamma} P_T^{1\gamma}}{1+\tau}. \quad (9)$$

Using these we can rewrite  $d\sigma^{1\gamma}/d\Omega_e$  as

$$\begin{aligned} \frac{d\sigma^{1\gamma}}{d\Omega_e} &= \frac{d\sigma_0^{1\gamma}}{d\Omega_e} + h \left[ \frac{d(\Delta\sigma_L^{1\gamma})}{d\Omega_e} (\hat{n}_{p'} \cdot \hat{z}) \right. \\ &\quad \left. + \frac{d(\Delta\sigma_T^{1\gamma})}{d\Omega_e} (\hat{n}_{p'} \cdot \hat{x}) \right]. \end{aligned} \quad (10)$$

Hence, the ratio of the form factors is given by:

$$\begin{aligned} R &= \frac{G_E}{G_M} = -\frac{P_T^{1\gamma}}{P_L^{1\gamma}} \frac{E_e + E'_e}{2M_p} \tan \frac{\theta_e}{2} \\ &= -\frac{d(\Delta\sigma_T^{1\gamma})/d\Omega_e}{d(\Delta\sigma_L^{1\gamma})/d\Omega_e} \frac{E_e + E'_e}{2M_p} \tan \frac{\theta_e}{2}. \end{aligned} \quad (11)$$

The contribution of the two photon exchange diagrams to the electron-proton elastic scattering cross section can be written as

$$\frac{d\sigma^{2\gamma}}{d\Omega_e} = \frac{2Re(\overline{\mathcal{M}}_0^* \mathcal{M}_{2\gamma}) E_e'^2}{64M_p^2 \pi^2 E_e^2} + \mathcal{O}(\alpha^4), \quad (12)$$

where  $\mathcal{M}_{2\gamma}$  is the total amplitude of the two photon exchange diagrams. As in the case of tree level process we can define  $d(\Delta\sigma_L^{2\gamma})/d\Omega_e$  and  $d(\Delta\sigma_T^{2\gamma})/d\Omega_e$  from the terms in  $d\sigma^{2\gamma}/d\Omega_e$  that are proportional to  $h(\hat{n}_{p'} \cdot \hat{z})$  and  $h(\hat{n}_{p'} \cdot \hat{x})$  respectively. Then,

$$\begin{aligned} \frac{d\sigma^{2\gamma}}{d\Omega_e} &= \frac{d\sigma_0^{2\gamma}}{d\Omega_e} + \frac{d(\Delta\sigma_N^{2\gamma})}{d\Omega_e} (\hat{n}_{p'} \cdot \hat{y}) \\ &\quad + h \left[ \frac{d(\Delta\sigma_L^{2\gamma})}{d\Omega_e} (\hat{n}_{p'} \cdot \hat{z}) + \frac{d(\Delta\sigma_T^{2\gamma})}{d\Omega_e} (\hat{n}_{p'} \cdot \hat{x}) \right]. \end{aligned} \quad (13)$$

Here  $d\sigma_0^{2\gamma}/d\Omega_e$  represents the terms independent of the spin of the final proton and  $d(\Delta\sigma_N^{2\gamma})/d\Omega_e$  corresponds to the normal polarization of the final proton.

Experimentally the polarization components,  $P_L$  and  $P_T$  are measured for different  $q^2$ . From these the ratio of the form factors is extracted by the following relation:

$$R_E = -\frac{P_T}{P_L} \frac{E_e + E'_e}{2M_p} \tan \frac{\theta_e}{2}. \quad (14)$$

In the tree level approximation  $R_E$  is identical to  $R$ . Let  $\tilde{G}_M$  be the experimentally measured value of  $G_M$ . Then,

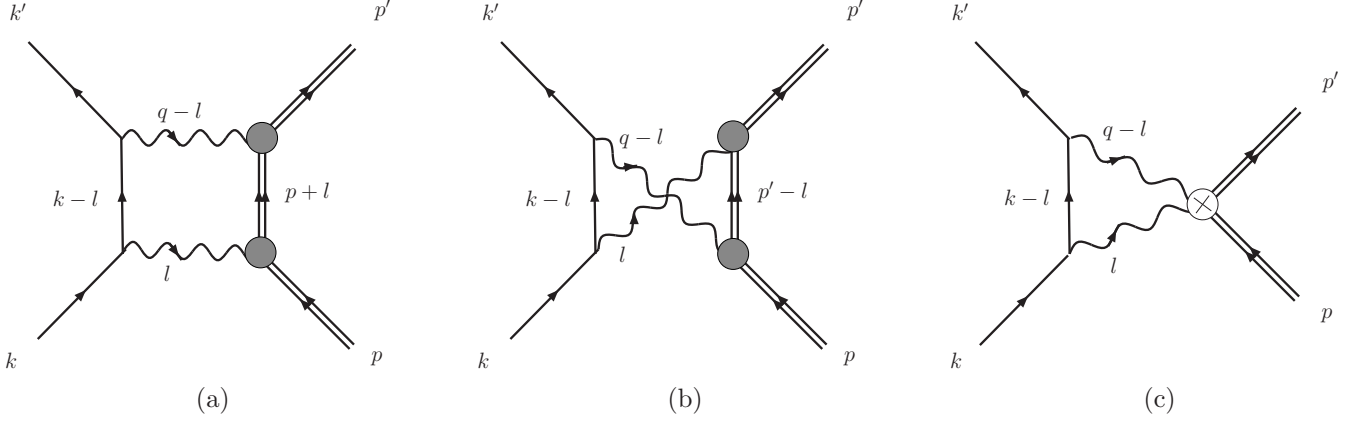


Figure 2: The two-photon exchange diagrams contributing to the elastic electron proton scattering: (a) box diagram, (b) cross-box diagram and (c) diagram proportional to  $\bar{b}^2$ . Another diagram proportional to  $\bar{b}^2$  is obtained by interchanging  $l \leftrightarrow (q-l)$  in (c)

with the knowledge of  $\tilde{G}_M$  and  $R_E$  one can define the following quantities:

$$\frac{d(\Delta\sigma_L)}{d\Omega_e} = \left( \frac{\alpha^2 E'_e \cos^2 \frac{\theta_e}{2}}{8E_e^3 \sin^4 \frac{\theta_e}{2}} \right) \frac{I_0 P_L}{1+\tau}, \quad (15)$$

$$\frac{d(\Delta\sigma_T)}{d\Omega_e} = \left( \frac{\alpha^2 E'_e \cos^2 \frac{\theta_e}{2}}{8E_e^3 \sin^4 \frac{\theta_e}{2}} \right) \frac{I_0 P_T}{1+\tau} \quad (16)$$

where

$$I_0 P_L = \frac{E_e + E'_e}{M_p} \sqrt{\tau(1+\tau)} \tilde{G}_M^2 \tan^2 \frac{\theta_e}{2}, \quad (17)$$

$$I_0 P_T = -2\sqrt{\tau(1+\tau)} \tilde{G}_M^2 R_E \tan \frac{\theta_e}{2}. \quad (18)$$

From these one obtains the ratio  $\bar{R}$  corrected for the two-photon exchange processes by the following relation:

$$\bar{R} = - \left[ \frac{d(\Delta\sigma_T)/d\Omega_e - d(\Delta\sigma_T^{2\gamma})/d\Omega_e}{d(\Delta\sigma_L)/d\Omega_e - d(\Delta\sigma_L^{2\gamma})/d\Omega_e} \right] \times \frac{E_e + E'_e}{2M_p} \tan \frac{\theta_e}{2} \quad (19)$$

$$= R_E \frac{1 - \Delta_T}{1 - \Delta_L} \quad (20)$$

where

$$\Delta_T = \frac{d(\Delta\sigma_T^{2\gamma})/d\Omega_e}{d(\Delta\sigma_T)/d\Omega_e}, \quad (21)$$

$$\Delta_L = \frac{d(\Delta\sigma_L^{2\gamma})/d\Omega_e}{d(\Delta\sigma_L)/d\Omega_e}. \quad (22)$$

## 2 Calculations and Results

As explained in [16] there are three diagrams that contribute in the two-photon exchange processes. Figs. 2(a)

and (b) show the box and cross-box diagrams respectively and Fig. 2(c) shows a diagram proportional to  $\bar{b}^2$ . The amplitudes for the box and cross-box diagrams are given by:

$$i\mathcal{M}_B = e^4 \int \frac{d^4 l}{(2\pi)^4} \left[ \frac{\bar{u}(k') \gamma^\mu (\not{k} - \not{l}) \gamma^\nu u(k, s_k)}{((k-l)^2 - m_e^2 + i\xi)} \right] \times \left[ \frac{1}{(l^2 - \mu^2 + i\xi)(\tilde{q}^2 - \mu^2 + i\xi)} \right] \times \left[ \bar{U}(p', s_{p'}) \left\{ F_1(\tilde{q}) \gamma_\mu + i \frac{\kappa_p}{2M_p} F_2(\tilde{q}) \sigma_{\mu\alpha} \tilde{q}^\alpha \right\} \right] \times \left[ \frac{\not{p} + \not{l} + M_p}{(p+l)^2 - M_p^2 + i\xi} \right] \times \left[ F_1(l) \gamma_\nu + i \frac{\kappa_p}{2M_p} F_2(l) \sigma_{\nu\beta} l^\beta \right] U(p), \quad (23)$$

$$i\mathcal{M}_{CB} = e^4 \int \frac{d^4 l}{(2\pi)^4} \left[ \frac{\bar{u}(k') \gamma^\mu (\not{k} - \not{l}) \gamma^\nu u(k, s_e)}{(k-l)^2 - m_e^2 + i\xi} \right] \times \left[ \frac{1}{(l^2 - \mu^2 + i\xi)(\tilde{q}^2 - \mu^2 + i\xi)} \right] \times \left[ \bar{U}(p', s_{p'}) \left\{ F_1(l) \gamma_\nu + i \frac{\kappa_p}{2M_p} F_2(l) \sigma_{\nu\beta} l^\beta \right\} \right] \times \left[ \frac{\not{p} + \not{\tilde{q}} - \not{l} + M_p}{(p+\tilde{q})^2 - M_p^2 + i\xi} \right] \times \left[ F_1(\tilde{q}) \gamma_\mu + i \frac{\kappa_p}{2M_p} F_2(\tilde{q}) \sigma_{\mu\alpha} \tilde{q}^\alpha \right] U(p). \quad (24)$$

Here  $\tilde{q} = q-l$  and  $\xi$  is an infinitesimal positive parameter. The amplitude for the diagram proportional to  $\bar{b}^2$  can be

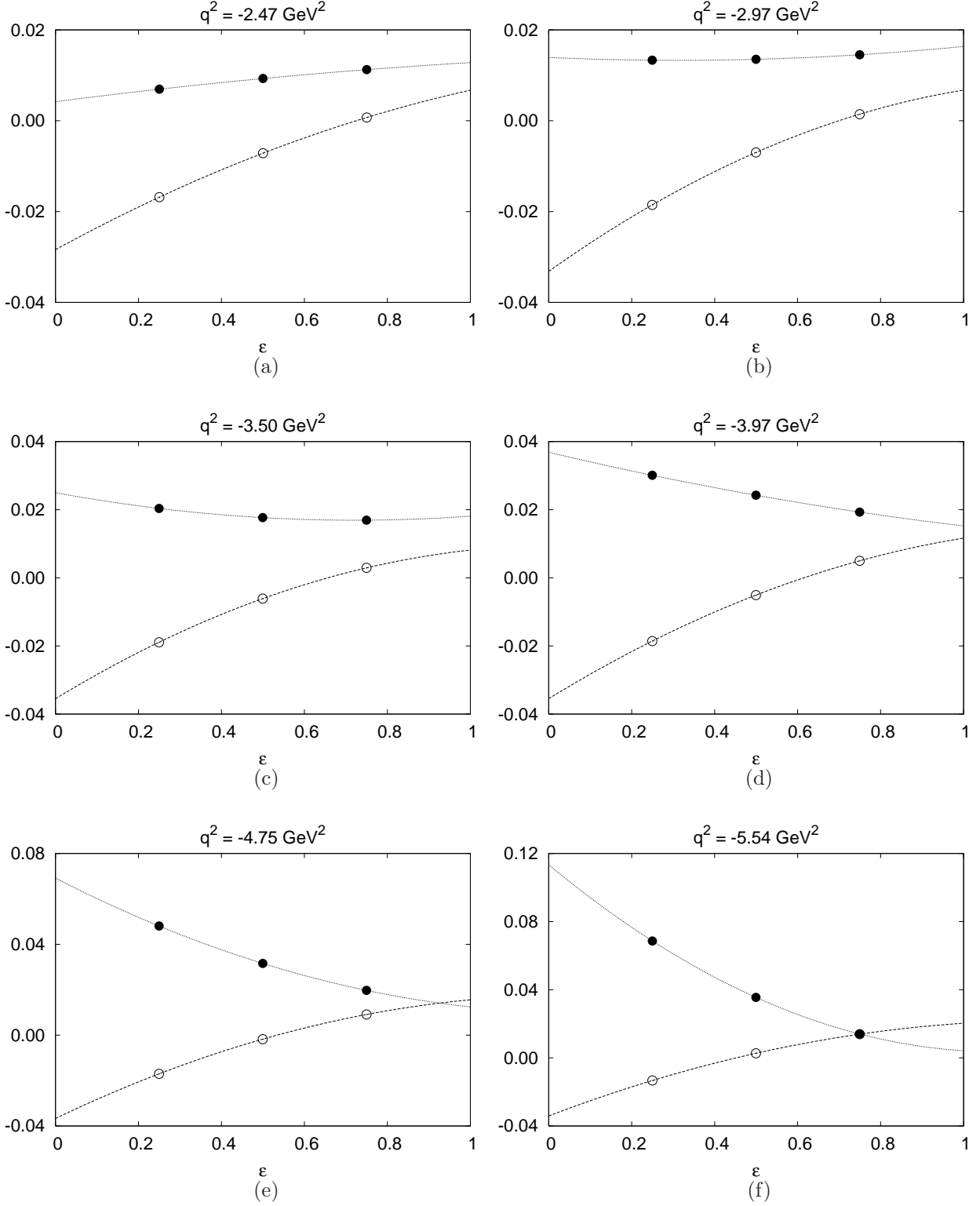


Figure 3: Contribution of box and cross-box diagrams to  $\Delta_L$  (unfilled circles) and  $\Delta_T$  (filled circles) for different  $q^2$  - (a)  $q^2 = -2.47 \text{ GeV}^2$ , (b)  $q^2 = -2.97 \text{ GeV}^2$ , (c)  $q^2 = -3.50 \text{ GeV}^2$ , (d)  $q^2 = -3.97 \text{ GeV}^2$ , (e)  $q^2 = -4.75 \text{ GeV}^2$ , (f)  $q^2 = -5.54 \text{ GeV}^2$ .  $\Delta_T$  is defined in (21) and  $\Delta_L$  is defined in (22).

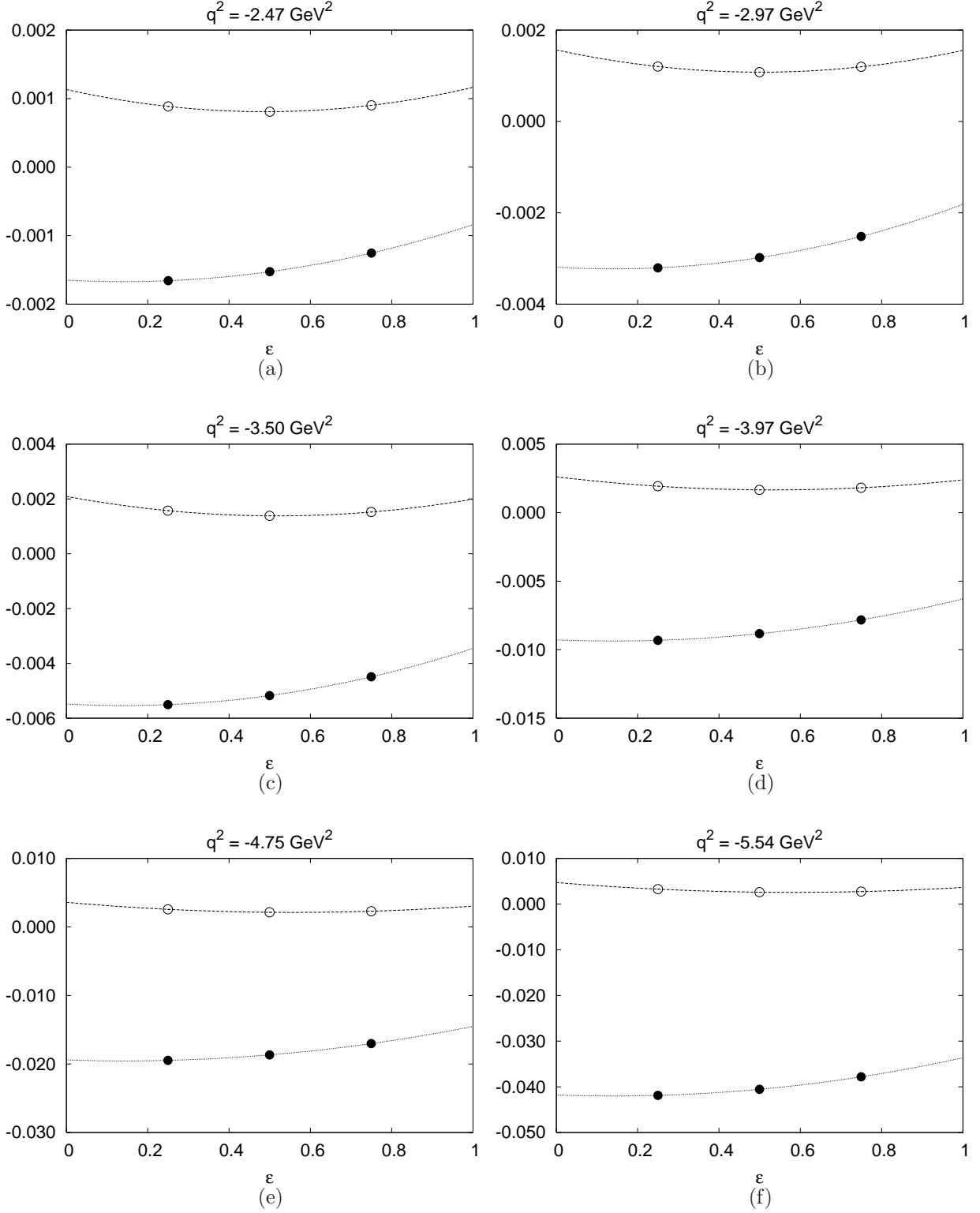


Figure 4: Contribution of the diagrams proportional to  $\bar{b}^2$  to  $\Delta_L$  (unfilled circles) and  $\Delta_T$  (filled circles) for different  $q^2$  - (a)  $q^2 = -2.47 \text{ GeV}^2$ , (b)  $q^2 = -2.97 \text{ GeV}^2$ , (c)  $q^2 = -3.50 \text{ GeV}^2$ , (d)  $q^2 = -3.97 \text{ GeV}^2$ , (e)  $q^2 = -4.75 \text{ GeV}^2$ , (f)  $q^2 = -5.54 \text{ GeV}^2$ .  $\Delta_T$  is defined in (21) and  $\Delta_L$  is defined in (22). Here  $\bar{b} = 1$ .

written as:

$$\begin{aligned}
i\mathcal{M}_{\bar{b}} = & \left( \frac{e^4 \bar{b}^2}{8M_p^2} \right) \int \frac{d^4 l}{(2\pi)^4} \left[ \frac{\bar{u}(k') \gamma^\mu (\not{k} - \not{l}) \gamma^\nu u(k, s_e)}{(k-l)^2 - m_e^2 + i\xi} \right] \\
& \times \left[ \frac{1}{(l^2 - \mu^2 + i\xi)(\tilde{q}^2 - \mu^2 + i\xi)} \right] \\
& \times \left[ \bar{U}(p', s_{p'}) \left\{ \left( \frac{i\kappa_p}{2M_p} F_2(\tilde{q}) \sigma_{\mu\alpha} \tilde{q}^\alpha \right) (\not{p} + \not{l} - M_p) \right. \right. \\
& \times \left( \frac{i\kappa_p}{2M_p} F_2(l) \sigma_{\nu\beta} l^\beta \right) + \left. \left. \left( \frac{i\kappa_p}{2M_p} F_2(l) \sigma_{\nu\beta} l^\beta \right) \right. \right. \\
& \left. \left. \times (\not{p} + \not{q} - \not{l} - M_p) \left( \frac{i\kappa_p}{2M_p} F_2(\tilde{q}) \sigma_{\mu\alpha} \tilde{q}^\alpha \right) \right\} U(p) \right]. \tag{25}
\end{aligned}$$

The total two photon exchange amplitude,

$$\mathcal{M}_{2\gamma} = \mathcal{M}_B + \mathcal{M}_{CB} + \mathcal{M}_{\bar{b}}. \tag{26}$$

In the numerical calculation we have dropped  $m_e$ . The model used for the form factors [17, 18] is the same as Model I described in [16]. The values of the parameters are repeated here in Appendix A for convenience. The results of our calculation may show some dependence on the precise form factor model. This appears to be the main uncertainty in our calculation which we hope to explore in a future publication.

Contributions from box and cross-box diagrams are computed at 10 different values of  $\mu^2$  (from 0.005 to 0.0095) for each value of  $q^2$  and  $\varepsilon$ . The cross-box diagram is well defined but for the evaluation of the box diagram a small imaginary term  $\xi$  is kept in the propagators. This makes the integral in the infrared limit well defined in the case  $m_e = 0$ . For each value of  $q^2$ ,  $\varepsilon$  and  $\mu^2$  we have calculated the box diagram amplitude for 4 different values of  $\xi$  (between 0.001 and 0.00175). The final  $\mu^2$  dependent box diagram amplitudes are obtained by extrapolation to  $\xi = 0$ . The diagram proportional  $\bar{b}^2$  has no infrared (IR) divergent term. So the contribution coming from it is computed keeping  $\mu^2 = 0$ .

Following Mo and Tsai [19, 20, 21, 22] one can show that in the limit  $\mu^2 \rightarrow 0$  the leading term from the box and cross-box diagram can be expressed as:

$$\mathcal{M}_{\text{IR}}^{2\gamma} = \frac{\alpha}{\pi} [K(p', k) - K(p, k)] \mathcal{M}_0, \tag{27}$$

where

$$\begin{aligned}
K(p_i, p_j) = & (p_i \cdot p_j) \int_0^1 \frac{dx}{(xp_i + (1-x)p_j)^2} \\
& \times \ln \left[ \frac{(xp_i + (1-x)p_j)^2}{\mu^2} \right].
\end{aligned}$$

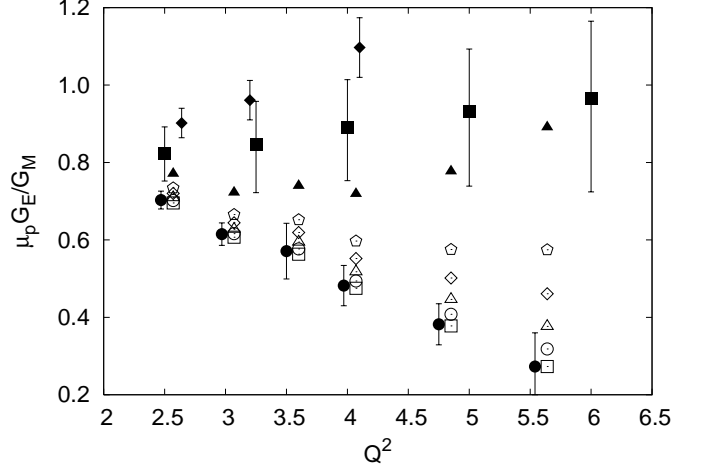


Figure 5: The ratio  $\mu_p G_E/G_M$  from polarization transfer experiments (filled circles) and after correction for the two-photon exchange diagrams with  $\bar{b} = 0$  (unfilled squares),  $\bar{b} = 2$  (unfilled circles),  $\bar{b} = 3$  (unfilled triangles),  $\bar{b} = 4$  (unfilled diamonds),  $\bar{b} = 5$  (unfilled pentagon) and  $\bar{b} = 6.91$  (filled triangles). The corrected values have been offset by  $\Delta Q^2 = 0.1 \text{ GeV}^2$  for clarity. The filled diamonds and the filled squares represent the Rosenbluth extraction experiment results obtained at JLAB and SLAC respectively.

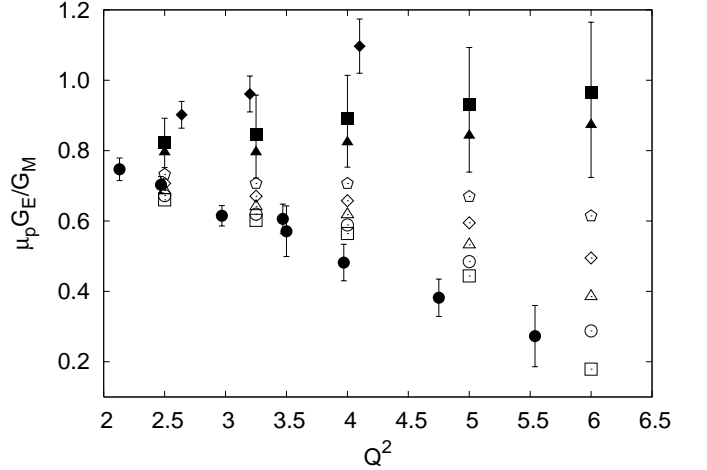


Figure 6: The ratio  $\mu_p G_E/G_M$  from SLAC Rosenbluth extraction experiments (filled squares) and after correction for the (unpolarized) two-photon exchange diagrams with  $\bar{b} = 0$  (unfilled squares),  $\bar{b} = 2$  (unfilled circles),  $\bar{b} = 3$  (unfilled triangles),  $\bar{b} = 4$  (unfilled diamonds),  $\bar{b} = 5$  (unfilled pentagon) and  $\bar{b} = 6.91$  (filled triangles). The filled diamonds represent the JLAB Rosenbluth extraction experiment results and the filled circles represent the results of the polarization transfer experiments.

Hence, the leading contributions to the cross sections coming from the box and cross-box diagrams are given by:

$$\left. \frac{d(\Delta\sigma_{\text{L,T}}^{2\gamma})}{d\Omega_e} \right|_{\text{IR}} = \frac{2\alpha}{\pi} [K(p', k) - K(p, k)] \frac{d(\Delta\sigma_{\text{L,T}}^{1\gamma})}{d\Omega_e}. \tag{28}$$

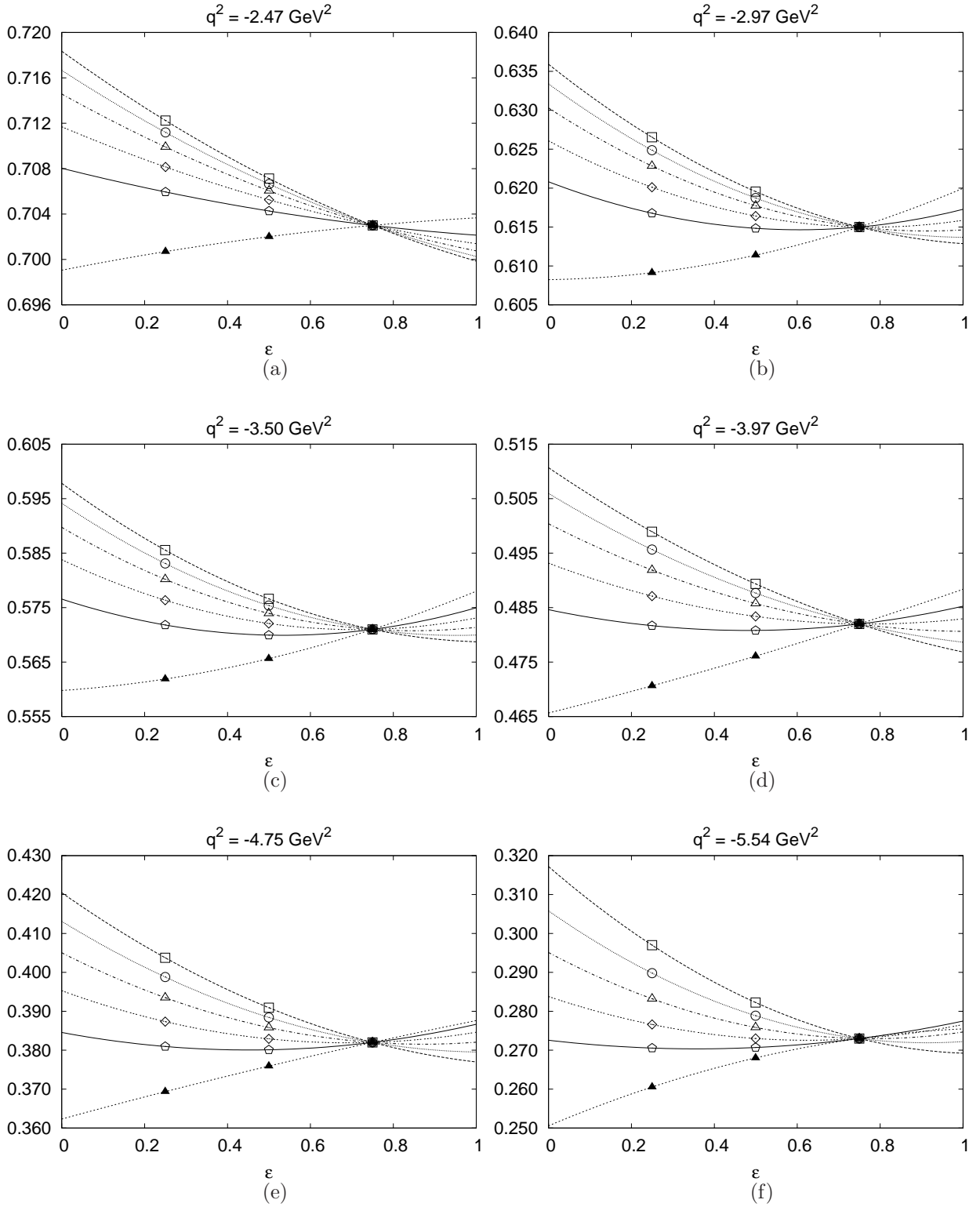


Figure 7: Dependence of the form factor ratio  $\mu_p G_E / G_M$  on  $\varepsilon$  from different  $q^2$  - (a)  $q^2 = -2.47 \text{ GeV}^2$ , (b)  $q^2 = -2.97 \text{ GeV}^2$ , (c)  $q^2 = -3.50 \text{ GeV}^2$ , (d)  $q^2 = -3.97 \text{ GeV}^2$ , (e)  $q^2 = -4.75 \text{ GeV}^2$ , (f)  $q^2 = -5.54 \text{ GeV}^2$ . For each  $q^2$ , the ratio,  $\mu G_E / G_M$  is plotted for different  $\bar{b}$  values -  $\bar{b} = 0$  (unfilled squares),  $\bar{b} = 2$  (unfilled circles),  $\bar{b} = 3$  (unfilled triangles),  $\bar{b} = 4$  (unfilled diamonds),  $\bar{b} = 5$  (unfilled pentagon) and  $\bar{b} = 6.91$  (filled triangles).

Let

$$\left. \frac{d(\Delta\sigma_{L,T}^{2\gamma})}{d\Omega_e} \right|_{\text{IR}} \equiv a_{L,T}^{ir} + b_{L,T}^{ir} \ln \mu^2. \quad (29)$$

To remove the IR part from  $d(\Delta\sigma_{L,T}^{2\gamma})/d\Omega_e$  we fit these with the following functions:

$$\frac{d(\Delta\sigma_{L,T}^{2\gamma})}{d\Omega_e} = a_{L,T}(\mu^2) + b_{L,T}(\mu^2) \ln \mu^2 \quad (30)$$

with

$$\begin{aligned} a_{L,T}(\mu^2) &= a_{L,T}^0 + a_{L,T}^1 \mu^2 + \mathcal{O}[\mu^4] \\ b_{L,T}(\mu^2) &= b_{L,T}^{ir} + b_{L,T}^1 \mu^2 + \mathcal{O}[\mu^4]. \end{aligned}$$

Hence,  $a_{L,T}^0$  give the IR removed  $d(\Delta\sigma_{L,T}^{2\gamma})/d\Omega_e$ .

Fig. 3 shows the contribution to  $\Delta_{L,T}$  coming from box and cross-box diagrams for different  $q^2$ . The contribution from the diagram proportional to  $\bar{b}^2$  is shown in Fig. 4. Fig. 5 shows the ratio  $\mu_p G_E/G_M$  from polarization transfer experiments (filled circles) and after correction for the two-photon exchange diagrams with  $\bar{b} = 0$  (unfilled squares),  $\bar{b} = 2$  (unfilled circles),  $\bar{b} = 3$  (unfilled triangles),  $\bar{b} = 4$  (unfilled diamonds),  $\bar{b} = 5$  (unfilled pentagon) and  $\bar{b} = 6.91$  (filled triangles). The highest value of  $\bar{b}$  used is obtained from the limit on nonlinearity of JLAB Rosenbluth data (see Section 3). In the range  $3.5 \geq Q^2 \geq 2.5 \text{ GeV}^2$ , the polarization transfer experiment used the kinematic regime with  $\varepsilon$  lying roughly between 0.7 and 0.8 [5]. For simplicity, here we assume a fixed value  $\varepsilon = 0.75$ . Fig. 6 shows the effect of  $\bar{b}$  on the unpolarized SLAC data. The method used to obtain these corrections is described in Section 6 of [16].

The form factor ratio  $G_E/G_M$  depends only on  $Q^2$ . However the ratio  $R_E$ , defined in (14), may show a dependence on  $\varepsilon$  due to higher order contributions. We predict this dependence by assuming that the electron-proton elastic scattering cross section can be well approximated by including only one and two photon exchange diagrams. The uncorrected form factor ratio  $R_E$  can be calculated by using (20), where the corrected ratio  $\bar{R}$  is independent of  $\varepsilon$ . Fig. 7 shows the predicted dependance of the uncorrected form factor ratio  $\mu_p R_E$  on  $\varepsilon$  for different  $\bar{b}$  and  $q^2$ . Here again we have assumed that the kinematic regime of the polarization transfer experiment corresponds to a fixed  $\varepsilon = 0.75$ . This may be used in future to fix the value of the parameter  $\bar{b}$ .

### 3 Limit on $\bar{b}$

As described in [16]  $\bar{b}$  is a free parameter. But the fact that  $\sigma_R^{\bar{b}}$  varies nonlinearly with  $\varepsilon$  allows us to put a limit on  $\bar{b}$ . We fit the reduced cross-section for the scattering of

unpolarized electrons from protons,  $\sigma_R$  with the following function:

$$\sigma_R = \mathcal{P}_0 + \mathcal{P}_1 \bar{\varepsilon} + \mathcal{P}_2 \bar{\varepsilon}^2, \quad (31)$$

where  $\bar{\varepsilon} = \varepsilon - \frac{1}{2}$ . As the result obtained by JLAB [23, 24] contains much smaller error-bars than the SLAC data we use JLAB data to obtain  $\mathcal{P}_2$  for different  $Q^2 = -q^2$ . Then we fit the contribution of the box and cross-box diagrams ( $\sigma_R^{\text{BCB}}$ ) and the contribution proportional to  $\bar{b}^2$  ( $\sigma_R^{\bar{b}}$ ) to the reduced cross-section with similar functions, i.e.,

$$\sigma_R^{\text{BCB}} = \mathcal{R}_0^{\text{BCB}} + \mathcal{R}_1^{\text{BCB}} \bar{\varepsilon} + \mathcal{R}_2^{\text{BCB}} \bar{\varepsilon}^2, \quad (32)$$

$$\sigma_R^{\bar{b}} = \bar{b}^2 (\mathcal{R}_0^{\bar{b}} + \mathcal{R}_1^{\bar{b}} \bar{\varepsilon} + \mathcal{R}_2^{\bar{b}} \bar{\varepsilon}^2). \quad (33)$$

To put the limit on  $\bar{b}$  we first obtain a limit on the nonlinearity parameter  $\mathcal{P}_2$ . The 2 sigma limit is obtained by finding the largest value of  $-\mathcal{P}_2$  such that  $\chi^2$  deviates from its minimum value by 4 units. We consider the largest value of  $-\mathcal{P}_2$  since the two photon exchange contributions are found to give a negative value of  $\mathcal{P}_2$ . The parameters  $\mathcal{P}_0, \mathcal{P}_1$  are also allowed to vary while determining the maximum value allowed for  $-\mathcal{P}_2$ . The best fit value of  $\mathcal{P}_2$  and the 1 and 2 sigma limits are given in Table 1. The best fit values of  $\mathcal{R}_2^{\text{BCB}}$  and  $\mathcal{R}_2^{\bar{b}}$  are given in Table 2. Assuming that the dominant source of nonlinear behaviour are the box, cross-box and  $\bar{b}$  diagrams, we obtain the limit on  $\bar{b}^2$  by the following relation,

$$\bar{b}_{max}^2 = \frac{\mathcal{P}_{2limit} - \mathcal{R}_2^{\text{BCB}}}{\mathcal{R}_2^{\bar{b}}} \quad (34)$$

where  $\mathcal{P}_{2limit}$  is the one or two sigma limit on the parameter  $\mathcal{P}_2$ . From Table 1 we see that the most stringent limit on  $\bar{b}$  is obtained for  $Q^2 = 2.64 \text{ GeV}^2$  and is given by:  $|\bar{b}| \lesssim 6.91$ . The nonlinearity of the reduced cross section  $\sigma_R$  has also been computed in [25] using the GPD formalism.

$Q^2$ in GeV <sup>2</sup>	$\mathcal{P}_2$ best fit	$\mathcal{P}_2$ 1 sigma limit	$\mathcal{P}_2$ 2 sigma limit	$\bar{b}^2$ 2 sigma limit
2.64	2.02	-3.82	-9.64	47.74
3.20	1.10	-3.70	-8.52	70.61
4.10	2.68	-2.92	-8.48	152.93

Table 1: The best fit and the one and two sigma limit on the parameter  $\mathcal{P}_2$  (defined in (31)) for different  $Q^2$ . All values of  $\mathcal{P}_2$  have been scaled by  $10^4$ . The corresponding two sigma limit on the parameter  $\bar{b}^2$  is also given.



$Q^2$ in GeV <sup>2</sup>	$\mathcal{R}_2^{\text{BCB}}$	$\mathcal{R}_2^{\bar{b}}$
2.64	$-4.04 \times 10^{-4}$	$-11.73 \times 10^{-6}$
3.20	$-3.69 \times 10^{-4}$	$-6.84 \times 10^{-6}$
4.10	$-1.95 \times 10^{-4}$	$-4.27 \times 10^{-6}$

Table 2: Values of the fitting parameters  $\mathcal{R}_2^{\text{BCB}}$  (defined in (32)) and  $\mathcal{R}_2^{\bar{b}}$  (defined in (33)) for different  $Q^2$ .

## 4 Conclusion

We have computed the two photon exchange corrections to the proton electromagnetic form factor ratio  $\mu_p G_E/G_M$  using a gauge invariant nonlocal Lagrangian. The Lagrangian is truncated to dimension five operators and depends on one unknown parameter  $\bar{b}$ . The higher dimension operators are expected to give negligible contributions as long as the off-shellness of the proton propagator is small. The two photon exchange corrections to the ratio are found to be small as long as the parameter  $\bar{b} \sim 1$ . We impose a limit on this parameter by the predicted nonlinearity in the  $\varepsilon$  dependence of the unpolarized reduced cross section  $\sigma_R$  due to two photon exchange contributions. A two sigma limit is found to be  $|\bar{b}| < 6.91$ . For such large value of  $\bar{b}$  the corrections to the polarization transfer experiment are quite significant. The corrections are found to go in the right direction and make the polarization transfer results come very close to the SLAC Rosenbluth measurement of this ratio. Hence we find that for a wide range of values of  $\bar{b}$  the results of the two experiments agree within errors after including the two photon exchange contributions. We also predict an  $\varepsilon$  dependence of the ratio extracted from polarization transfer. This can be tested in future experiments and also be used to extract the value of the parameter  $\bar{b}$ .

## Appendix A Model for the Form Factors

The fits for  $G_M/\mu_p$  and  $G_E$  are given by:

$$\frac{G_M(q^2)}{\mu_p} = \sum_{a=1}^4 \frac{A'_a}{(q^2 - m_a^2 + im_a \Gamma'_a)} \quad (\text{A.1})$$

$$G_E(q^2) = \sum_{a=1}^6 \frac{B'_a}{(q^2 - m_a^2 + im_a \Gamma'_a)}. \quad (\text{A.2})$$

The values of the masses and the parameters are tabulated in Table 3. Using the fits for the magnetic and electric form factors one can determine the Dirac and Pauli form factors.

$a$	$A'_a$	$B'_a$	$m_a$	$\Gamma'_a$
1	-2.882564 +i 1.944314	-3.177877 +i 2.123389	0.8084	0.2226
2	2.882564 -i 1.944314	3.177877 -i 2.123389	0.9116	0.1974
3	-1.064011 -i 3.216318	-0.608148 -i 5.685885	1.274	0.5712
4	1.064011 +i 3.216318	0.608148 +i 5.685885	1.326	0.5488
5	0	3.211388 +i 0.693412	1.96	1.02
6	0	-3.211388 -i 0.693412	2.04	0.98

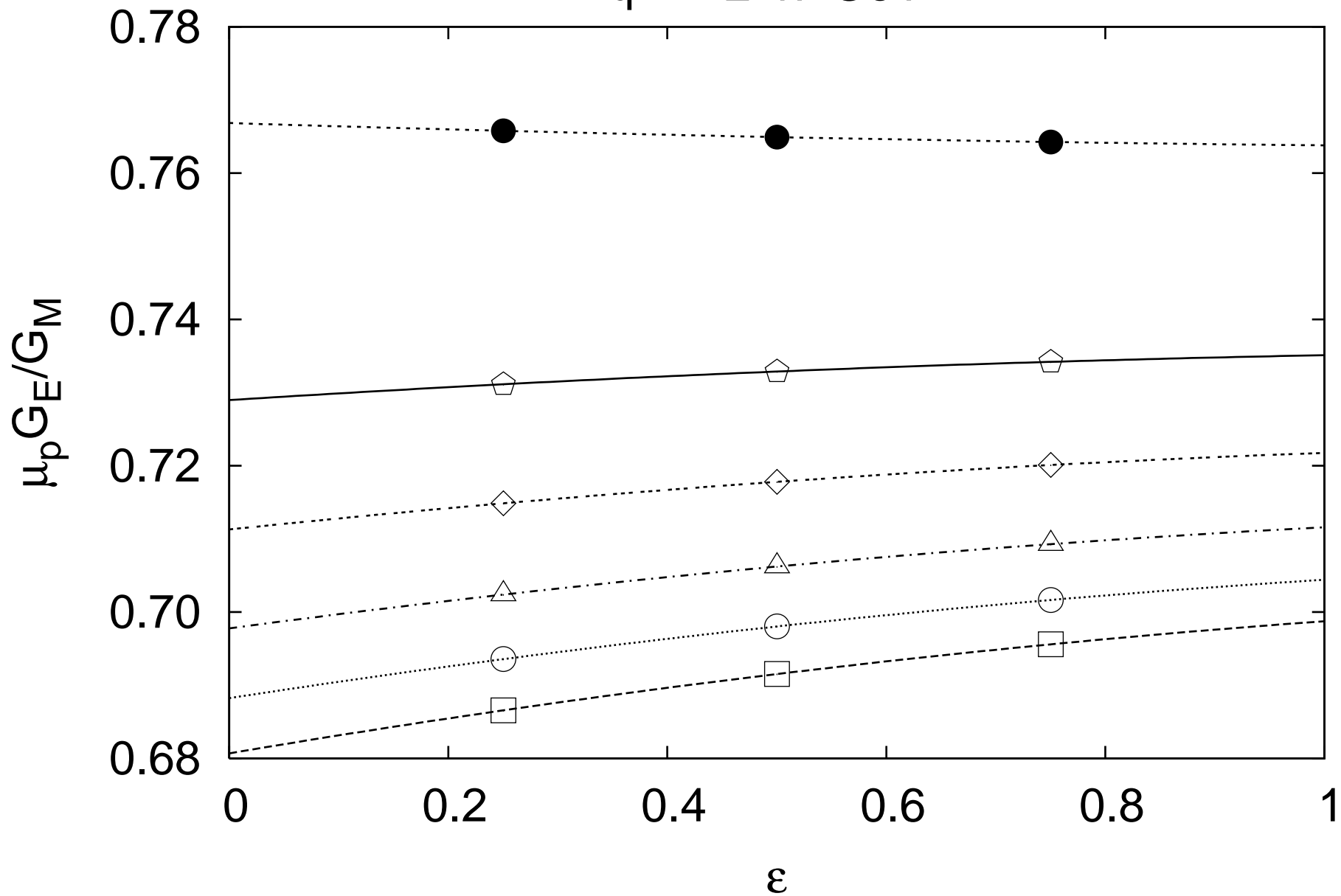
Table 3: Masses, widths and parameter values for  $G_M/\mu_p$  and  $G_E$  fits.  $A'_a$ 's and  $B'_a$ 's are defined in (A.1) and (A.2).

## References

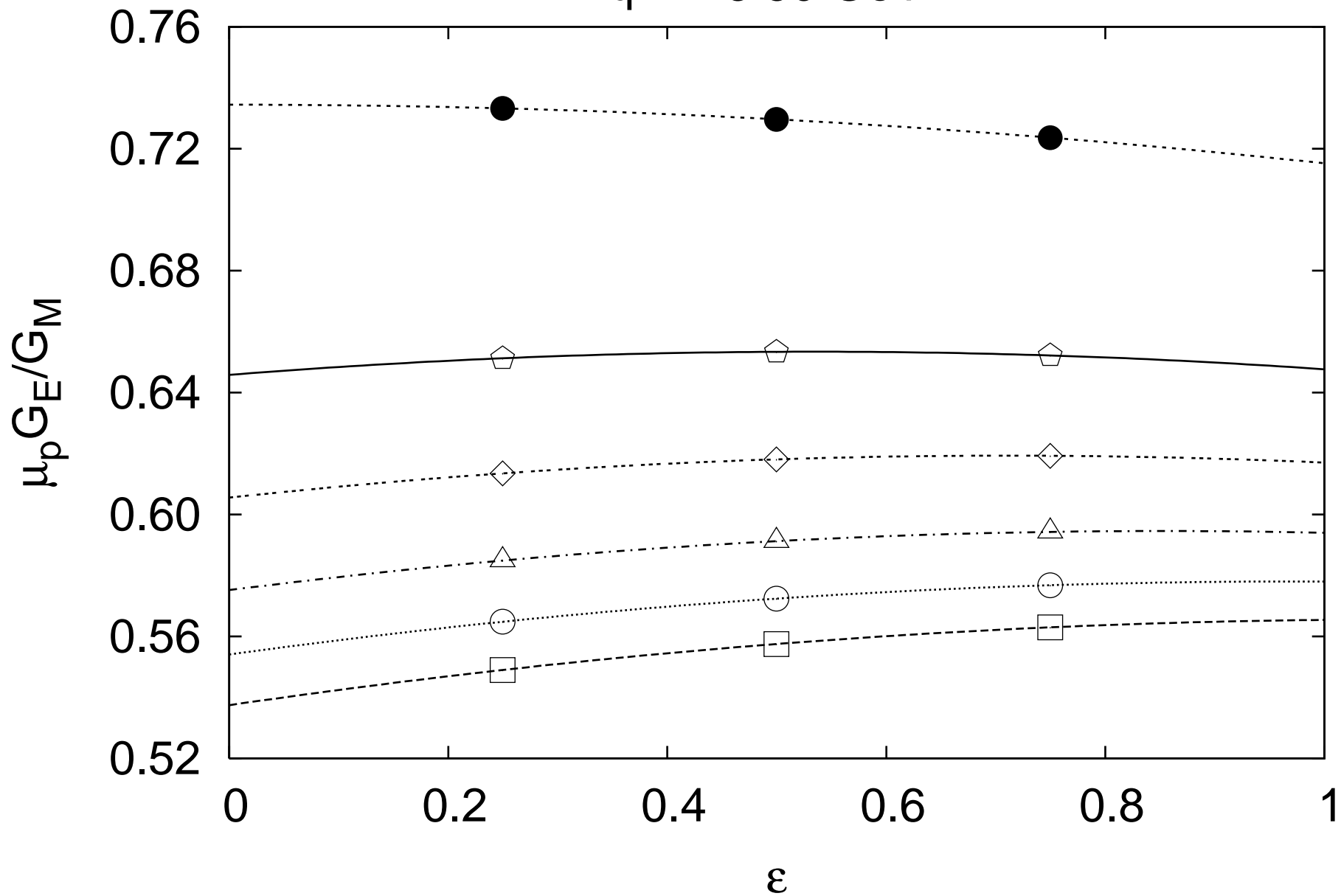
- [1] J. Arrington, C. D. Roberts, J. M. Zanotti, J. Phys. G **34**, S23 (2007); nucl-th/0611050.
- [2] C. F. Perdrisat, V. Punjabi, M. Vanderhaeghen, Prog. Part. Nucl. Phys. **59**, 694 (2007); hep-ph/0612014.
- [3] M. K. Jones *et al*, Phys. Rev. Lett. **84**, 1398 (2000).
- [4] O. Gayou *et al*, Phys. Rev. Lett. **88**, 092301, (2002).
- [5] V. Punjabi *et al*, Phys. Rev. **C 71**, 055202 (2005); Phys. Rev. **C 71**, 069902(E) (2005).
- [6] A. I. Akhiezer, L. N. Rosentsweig, I. M. Shmushkevich, Sov. Phys. JETP **6**, 588 (1958); J. Scofield, Phys. Rev. **113**, 1599 (1959); *ibid* **141**, 1352 (1966); N. Dombey, Rev. Mod. Phys. **41**, 236 (1969); A. I. Akhiezer and M. P. Rekalov, Sov. J. Part. Nucl. **4**, 277 (1974); R. G. Arnold, C. E. Carlson and F. Gross, Phys. Rev. **C 23**, 363 (1981).
- [7] R. C. Walker *et al.*, Phys. Rev. **D 49**, 5671 (1994).
- [8] L. Andivahis *et al.*, Phys. Rev. **D 50**, 5491 (1994).
- [9] M. N. Rosenbluth, Phys. Rev. **79**, 615 (1950).
- [10] P. A. M. Guichon and M. Vanderhaeghen, Phys. Rev. Lett. **91**, 142303 (2003).
- [11] J. Arrington, Phys. Rev. **C 71**, 015202 (2005); hep-ph/0408261.
- [12] P. G. Blunden, W. Melnitchouk and J. A. Tjon, Phys. Rev. Lett. **91**, 142304 (2003), nucl-th/0306076; P. G. Blunden, W. Melnitchouk and J. A. Tjon, Phys. Rev. **C 72** 034612 (2005), nucl-th/0506039.

- [13] A. V. Afanasev, S. J. Brodsky, C. E. Carlson, Yu-Chun Chen and M. Vanderhaeghen, Phys. Rev. **D 72** 013008 (2005), hep-ph/0502013.
- [14] M. P. Rekalo and E. Tomasi-Gustafsson, Eur. Phys. J. **A 22**, 331 (2004).
- [15] M. A. Belushkin, H. W. Hammer and U. G. Meissner, hep-ph/0705.3385.
- [16] P. Jain, S. D. Joglekar and S. Mitra, Eur. Phys. J. C **52**, 339 (2007) [arXiv:hep-ph/0606149].
- [17] R. Baldini et al, Eur. Phys. J. **C 11**, 709 (1999).
- [18] R. Baldini et al, Nucl. Phys. **A 755**, 286 (2005).
- [19] Y. S. Tsai, Phys. Rev. **122**, 1898 (1961).
- [20] L. M. Mo and Y. S. Tsai, Rev. Mod. Phys. **41**, 205 (1969).
- [21] L. C. Maximon and W. C. Parke, Phys. Rev. C **61**, 045502 (2000) [arXiv:nucl-th/0002057].
- [22] R. Ent *et al*, Phys. Rev. **C 64**, 054610-1 (2001).
- [23] I. A. Qattan *et al*, Phys. Rev. Lett. **94**, 142301 (2005); nucl-ex/0410010.
- [24] I. A. Qattan, nucl-ex/0610006.
- [25] Z. Abidin and C. E. Carlson, arXiv:0706.2611 [hep-ph].

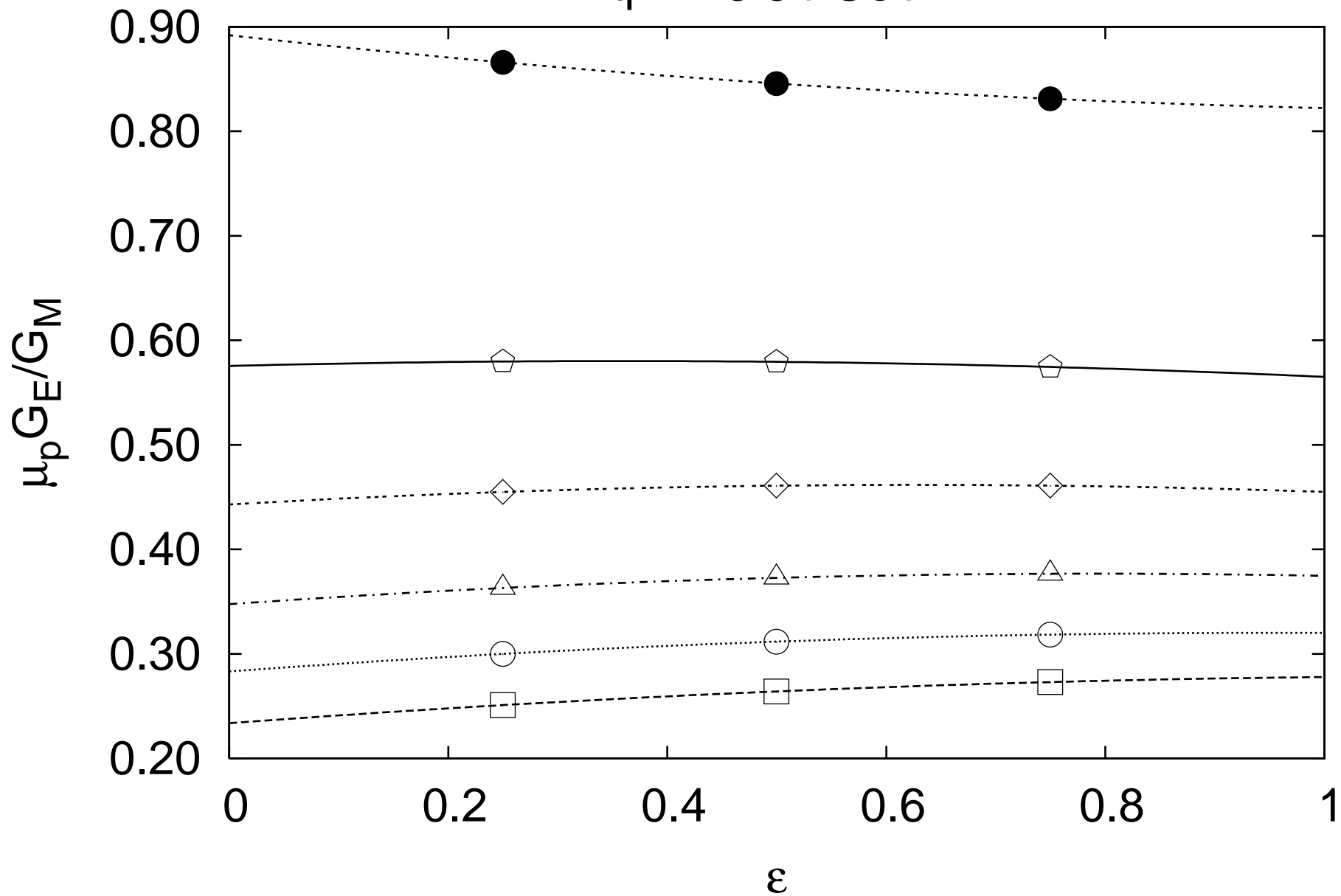
$q^2 = -2.47 \text{ GeV}^2$



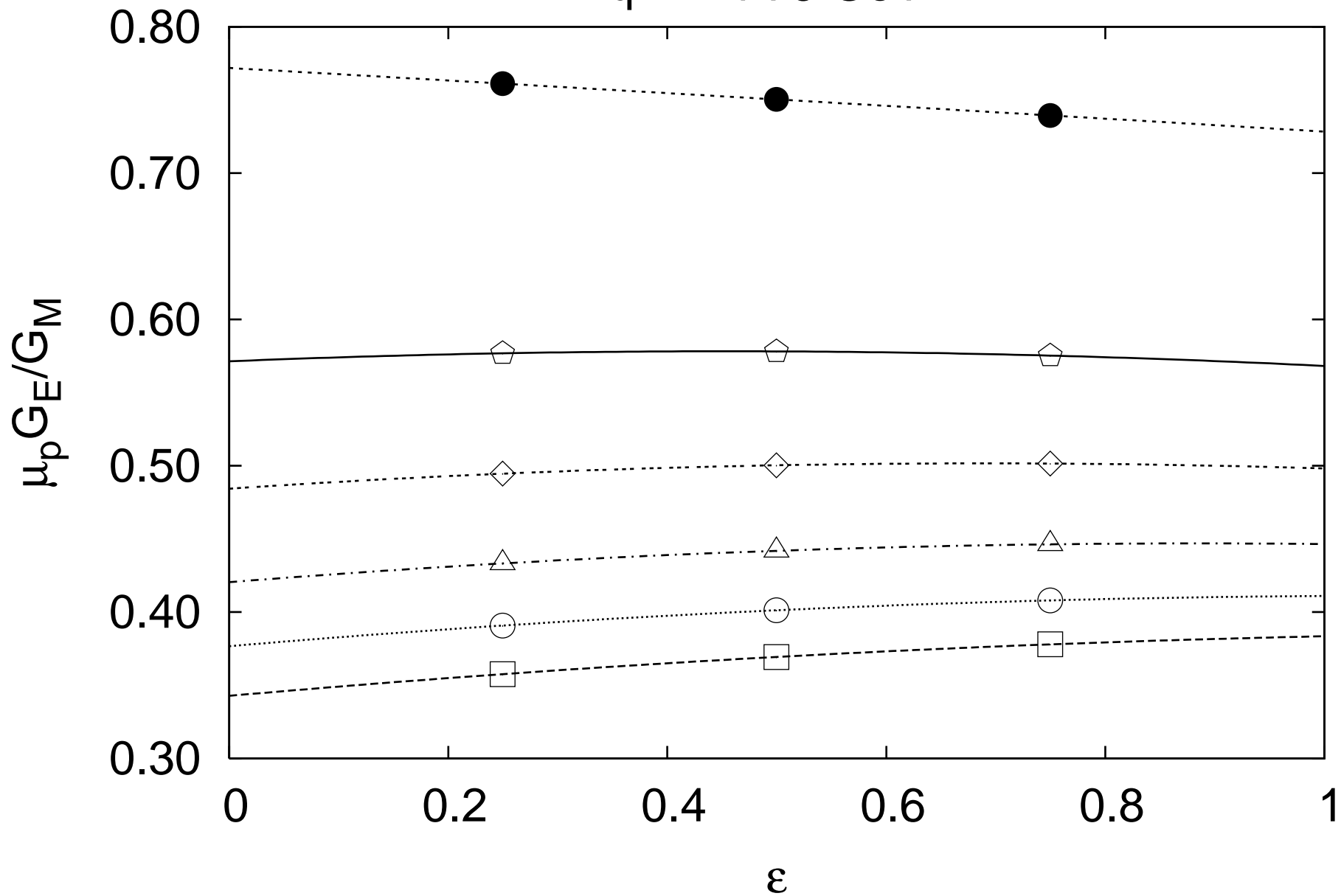
$q^2 = -3.50 \text{ GeV}^2$



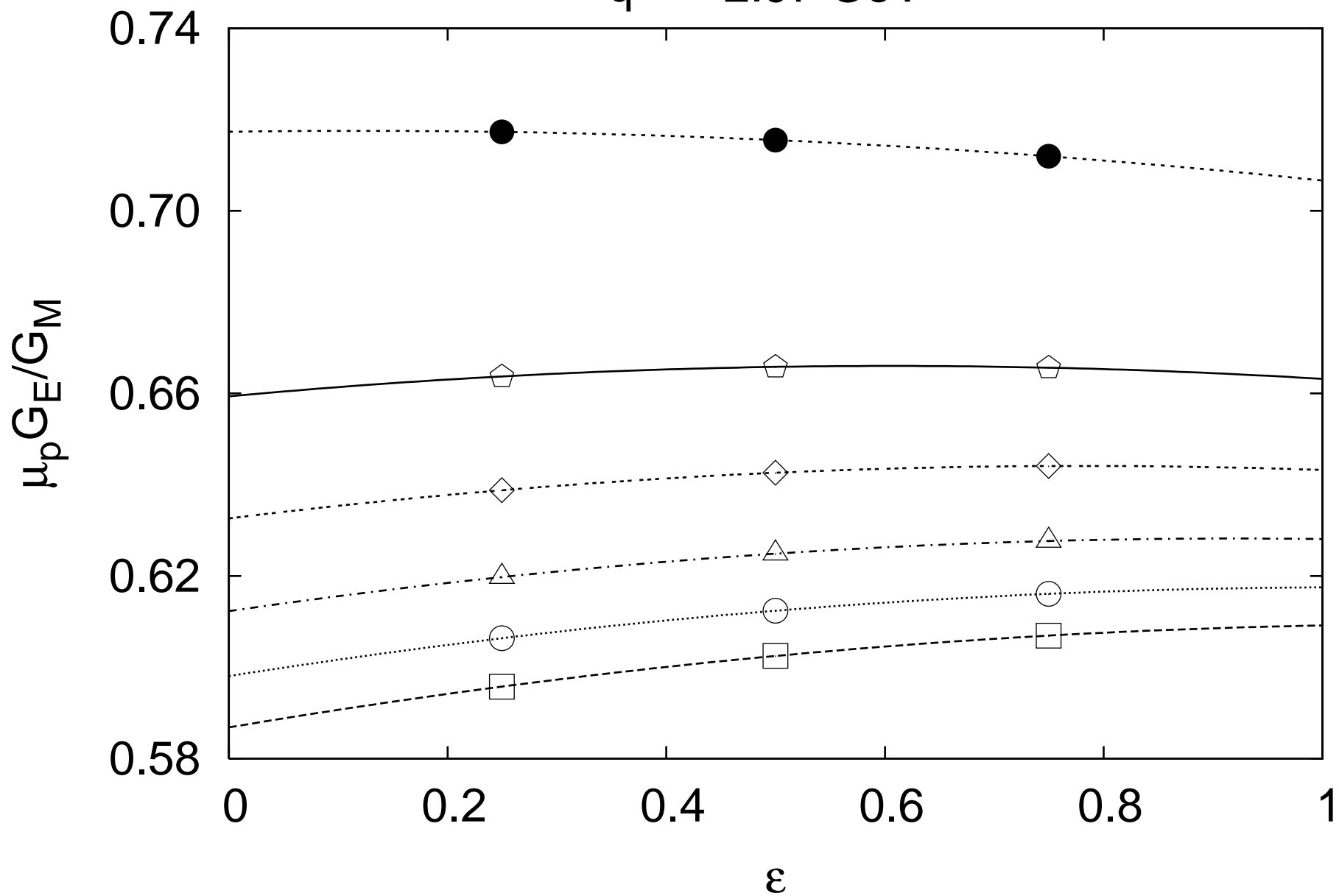
$q^2 = -5.54 \text{ GeV}^2$



$q^2 = -4.75 \text{ GeV}^2$



$q^2 = -2.97 \text{ GeV}^2$



$q^2 = -3.97 \text{ GeV}^2$

